The antifungal mechanism of the biogenic antimicrobial Ningnanmycin on *Didymella segeticola* involves binding to tryptophanyl-tRNA synthetase, inhibiting translation

Li Dongxue
Key Laboratory of Green Pesticide and Agricultural Bioengineering, Ministry of Education
Qiaoxiu Yin
Key Laboratory of Green Pesticide and Agricultural Bioengineering, Ministry of Education
Xue Wang
National Registration Authority for Agricultural and Veterinary Chemicals: Australian Pesticides and Veterinary Medicines Authority
Shilong Jiang
College of Agriculture, Guizhou University
Dissanayake Saman Pradeep Dharmasena
Key Laboratory of Green Pesticide and Agricultural Bioengineering, Ministry of Education
Xian Wu
National Registration Authority for Agricultural and Veterinary Chemicals: Australian Pesticides and Veterinary Medicines Authority
Delu Wang
College of Forestry, Guizhou University
Zhuo Chen (gychenzhuo@aliyun.com)
Key Laboratory of Green Pesticide and Agricultural Bioengineering, Ministry of Education
https://orcid.org/0000-0001-7130-8457

Research article

Keywords: Didymella segeticola, Ningnanmycin, Antifungal activity, Mycelial morphology, Transcriptional analysis, Action mechanism

Posted Date: November 24th, 2020

DOI: https://doi.org/10.21203/rs.3.rs-112823/v1

Abstract

Background

Tea [Camellia sinensis (L.) Kuntze] has been recently cultivated in Guizhou Province, China, where the cultivated area has reached 350,000 hectares, making it the major tea-growing region in world. Tea leaf spot caused by *Didymella segeticola* can induce the decreases in quality and quantity of tea leaves, which is an important disease in tea plantations at higher altitude, where cold spells occur in late spring. As a promising biogenic antimicrobial agent against crop diseases, Ningnanmycin (NNM) was produced from *Streptomyces noursei* var. *xichangensisn*, represented higher field efficiency against fungal, bacterial and viral phytopathogens, lower toxicity and lower residue. However, the action mechanism of NNM against phytopathogens just stays on the stage of anti-viral mechanism, which limits the application of NNM in the management of plant fungal diseases. Here, we studied the action mechanism of NNM against *D. segeticola* using many methods of transcriptome, ultrastructure, molecular biology and molecular docking.

Results

NNM strongly inhibited the mycelial growth of *D. segeticola* with the half-maximal effective concentration of 1287.54 U/mL. Optical, fluorescence, scanning and transmission electron microscopy were applied to observe morphological changes of cellular, organelle for *D. segeticola* treated by NNM. A great number of morphological changes of *D. segeticola* indicated that NNM could affect the biosynthesis of the phytopathogen. For further, RNA-Seq results showed that NNM treated *D. segeticola* induced 1,363 significantly differentially expressed genes (DEGs) comparing with the control ($P < 0.05$). The DEGs were highly enriched in structural component of ribosome, ribosome and translation by Gene Ontology, as well as in ribosome pathway at Kyoto Encyclopedia of Genes and Genomes. NNM regulated the mRNA levels of *RPS7*, *RPS9*, *RPS10b*, *RPL9*, *RPL11* and *TrpRS*, and represent the different regulation mode by the comparative analysis with a classical translation extension inhibitor, cycloheximide. The molecular docking indicated that NNM possessed a marked affinity with TrpRS, with the binding free energy is -101.55 kcal/mol.

Conclusions

NNM could potentially affect translation by binding to tryptophanyl-tRNA synthetase, thus inhibiting mycelial growth. This study will provide insights for anti-fungal mechanism of NNM and contribute to the control and prevention of tea leaf spot disease.

Background

Tea leaf spot is widespread throughout the areas worldwide where tea (*Camellia sinensis*) is grown, leading to large reductions in the production of tea leaves, and causing serious economic losses. So far, many fungal pathogens have been shown to cause tea leaf spot, such as *Lasiodiplodia theobromae* [1],

Didymella segeticola [2], *Epicoccum sorghinum* [3], *Didymella bellidis* [4], *Alternaria alternata* [5] and *Curvularia lunata* [6]. Leaf spot caused by *D. segeticola* is a recently discovered disease, which was found in Shiqian County, Guizhou Province in southwestern China, and identified by our research group [7]. The disease occurs widely in tea plantations at higher altitude, where cold spells occur in late spring [7]. The disease can cause decreases in the quality and quantity of tea because of the lack of effective control measures [7]. In recent years, leaf spot caused by *D. segeticola* was found in other tea regions in Guizhou Province, indicating that the disease is at risk of spreading. *D. segeticola* is a member in the clade of *Didymella in* the Didymellaceae family, which includes many phytopathogens, decreasing the commercial returns from crops [8].

For these reasons, it was very important to identify biogenic agents with activity against *D. segeticola* and to study the mode of action of successful candidate biogenic agents [7]. Ningnanmycin (NNM), a new type cytosine nucleoside peptide antibiotic, was developed by the Chengdu Institute of Biology, Chinese Academy of Sciences [9]. It is an antimicrobial agent with high effectiveness and low human toxicity, isolated from the fermented broth of the bacterium *Streptomyces noursei* var. *xichangensisn*, a recently discovered variant of *Streptomyces norkelii* [9] .Research showed that NNM has been able to protect against fungal, bacterial and viral phytopathogens in a range of crops, including rice bacterial blight and fungal diseases such as powdery mildews of wheat, vegetables [10]. NNM has also been reported to exhibit substantial antiviral activity on several phytopathogens, such as tobacco mosaic virus, capsicum mottle virus and cucumber mosaic virus [11–13]. The mode of action of NNM against virus has been reported that inhibiting TMV coat protein assembly, but few reports exist on its function against fungi [14]. Therefore, the antifungal mechanism of the broad-spectrum antimicrobial NNM is worthwhile studying.

In a previous study, we sequenced the whole genome of *D. segeticola* [15], integrated mRNA and small RNA of the pathogen and its host, tea during infection [16]. The annotated whole-genome sequence of the related *D. segeticola* will provide a resource for identifying trait-specific genes of the pathogen *D. segeticola*. In this study, we determined the antifungal activity of NNM against *D. segeticola* by the plating method and studied differential gene expression of *D. segeticola* in response to NNM by RNA-sequencing (RNA-Seq). Concurrently, we validated the expression levels of six genes involved in the translation process, using molecular methods. We used various microscopy techniques, including optical microscopy, fluorescence microscopy, scanning electron microscopy (SEM) and transmission electron microscopy (TEM) to explore the effects of NNM on the mycelial morphology and ultrastructure of *D. segeticola*. Molecular dicking was used to speculate the most promising target. This research aimed to evaluate the effect of NNM on *D. segeticola*, to elucidate the intracellular action sites and improve our understanding of the antifungal mechanism.

Results

Anti-fungal activity of NNM toward *D. segeticola* mycelial growth

The inhibitory effect of NNM on *D. segeticola* was evaluated at various NNM concentrations. Based on the diameter of the fungal colony, NNM exhibited a dosage-dependent inhibition rate, with the regression equation being y=0.8807x+2.2439 and R^2=0.9962, where y=inhibition rate and x=NNM concentration (U/mL), and the EC_{50} value was determined by regression to be 1287.54±111.53 U/mL (Fig. 1 and Additional file 4: Table S1). The inhibition rate of NNM also exhibited a greater inhibition activity toward mycelium dry weight than that based on colony diameter. For example, the dry weight inhibition rate was more than 80.0% at the EC_{50} NNM (Additional file 4: Table S1). Based on these two measures of bioactivity, we found that NNM could inhibit not only the increase in colony diameter but also mycelial biomass over time.

Effect of NNM on mycelial morphology of *D. segeticola*

The external walls of control hyphae of *D. segeticola* were smooth and the development of fresh hyphae, septa and cell walls, as viewed under an optical microscope, were normal (Fig. 2a and c). After the mycelia of *D. segeticola* were exposed *in vitro* to NNM in liquid culture, the morphological changes of hyphae, such as swelling, were dependent on treatment time. The hyphae were slightly swollen after exposure for 1 h (Fig. 2b, rectangles), but appeared to be further inflated when the treatment time was extended to 14 h, by which time the density of the cytoplasmic contents of the hyphae had decreased and granulations had appeared (Fig. 2d, black arrows). We speculated that NNM inhibited the growth of the fungus, by colony diameter or biomass, by inhibiting biosynthesis in the fungus.

Effect of NNM on cell nuclei and septa of *D. segeticola*

We investigated the cell nucleus distribution and septum development of *D. segeticola* by staining with DAPI (staining nuclei) and CFW (staining chitin) after treatment of the hyphae with NNM. First, analysis by fluorescence microscopy showed that the cell nuclei were regularly distributed in the control treatment (Fig. 3a, e and i), as indicated by arrows), whereas the distribution of cell nuclei in hyphae after treatment with the low concentrations of EC_{10} or EC_{30} NNM for 1 h was unregularly distributed (Fig. 3b and c). Furthermore, the cell nuclei in treated hyphae, exposed to the high concentration of EC_{50} for 1 h, were indistinct, with the fusion of several nuclei (Fig. 3d). When the treatment time was extended from 1 to 12 or 24 h, the changes in the cell nuclei were more obvious, especially at the concentration equivalent to EC_{50} (Fig. 3f to h and j to l). These results indicated that NNM detrimentally affected the organization and distribution of cell nuclei in *D. segeticola*.

When the hyphae of *D. segeticola* had not been treated with NNM, the internal structure was clear and complete (Fig. 4a, e and i). The cell septa of hyphae treated with low concentrations (EC_{10} and EC_{30}) of NNM for 1 h were similar to those of the control (Fig. 4b and c, arrow), whereas the septa of hyphae treated with the EC_{50} concentration for 1 h of NNM were thickened and the fluorescence intensity associated with CFW staining (specific for chitin and cellulose in cell walls) increased, compared with the control (Fig. 4d, arrow). When the treatment time was extended, the septa in hyphae treated with low concentrations (EC_{10}) of NNM for 12 or 24 h were thickened (Fig. 4f and j). Furthermore, the fluorescence

intensity of the cell septa and walls all increased (relative to the control hyphae) at the NNM concentrations EC_{30} or EC_{50} for exposure times of 12 or 24 h (Fig. 4g, h, k and l), with the structures being unclear. The results indicated that NNM appeared to affect the formation or development of septa, so that the increased staining of the cell nuclei or the cell septa indicated that NNM inhibited biosynthesis by the fungus, which, in turn, affected the normal growth of *D. segeticola*.

Effect of NNM on cell ultrastructure of *D. segeticola*

SEM showed that the control hyphae exhibited characteristic morphology, with healthy, robust and uniform growth (Fig. 5a, rectangles), and plump cell bodies and septa (Fig. 5a, circles), with the hyphal surface being smooth (Fig. 5a, rectangles). When *D. segeticola* was treated with NNM at EC_{50} for 1 h, the hyphae became abnormal, and the tips of the hyphae became inflated (Fig. 5b, rectangles). After 14 h, the hyphae were abnormal (Fig. 5c, circles), and the growth of new hyphae was inhibited, with individual hyphae being swollen compared with the control (Fig. 5c, rectangles). The results further verified that the growth and development of hyphae was detrimentally affected by NNM.

TEM showed that the control hyphae revealed high density cytoplasm with intact organelles (Fig. 6a to c), and the structure of the cell walls and plasma membranes (Fig. 6b). What' more, many lipid bodies were clearly evident (Fig. 6a and c). After treatment with NNM at the concentration-equivalent of EC_{50} for 1 h, the cytoplasm appeared degraded with empty spaces developed (Fig. 6d and e, asterisks). Moreover, the treated hyphae exhibited rough cell walls and cell septa and fewer lipid bodies (Fig. 6e and f). As the period of treatment with NNM increased, the cytoplasm became more degraded (Fig. 6g, asterisks) and many dense bodies appeared (Fig. 6g, black arrows). Some damaged organelles were apparent, such as mitochondria (Fig. 6h and i, red arrows). Meanwhile, the number of lipid bodies decreased, in comparison with the control hyphae. These results indicated that NNM inhibited biosynthesis in the fungus and disturb the information of biological substance.

Summary of sequences, assembly and functional annotation

In total, 43.18 Gb valid data were obtained from the transcriptome sequencing of mycelial samples from the two groups (*D. segeticola* treated by 0 U/mL and EC_{50} NNM for 1 h, respectively), ranging from 6.25 to 7.83 Gb per sample (Additional file 4: Table S2). A total of 44.64 Gb raw data were obtained. After removing the unqualified reads from the raw data, the Q20 of the valid data was above 99.91%, Q30 was above 97.99% and the GC proportion was 55% (Additional file 4: Table S2). Valid data in the six samples mapped to the reference genome were all at least 96.94%, unique mapped reads was at least 74.91% and multi-mapped reads were at least 19.78% (Additional file 4: Table S3). According to the region of the reference genome, valid data from six samples on the exon regions were all more than 96% (Additional file 4: Table S4). After assembly, a total of 10,894 genes were obtained from the six samples of the two different treatments, which were compared with Gene Ontology (GO) and Kyoto Encyclopedia of Genes and Genomes (KEGG) for annotation and analysis (Additional file 4: Table S5 and S6). Gene expression level was represented by fragments per kilobase of exon model per million mapped reads (FPKM)

(Additional file 1: Figure S1a and Additional file 4: Table S7). The number of expressed genes from the six samples was similar in each gene expression value region (Additional file 4: Table S8). The density distributions of gene expression in both control and treatment group were shown in Additional file 1: Figure S1b. All expressed genes of the three biological replicates for each group were shown in Additional file 4: Table S9.

GO and KEGG enrichment analysis of differentially expressed genes (DEGs)

The RNA-Seq analysis revealed 1,363 genes were significantly differentially expressed, including 743 up-regulated and 620 down-regulated genes (Additional file 2: Figure S2 and Additional file 4: Table S9). The GO enrichment analysis revealed that the DEGs were distributed across 1297 GO terms (Additional file 4: Table S10). The translation, ribosome and structural constituent of ribosome terms were significantly enriched in the level of Biological Process (BP), Cell Component (CC) and Molecular Function (MF), with significantly DEGs number of specific KEGG pathway (S gene numbers) being 54, 38, 56, respectively (Fig. 7a, purple histograms). Genes encoding tryptophanyl-tRNA synthetase (*TrpRS*), 60S ribosomal protein L9 (*RPL9*), 60S ribosomal protein L11 (*RPL11*), 40S ribosomal protein S7 (*RPS7*), 40S ribosomal protein S9 (*RPS9*) etc. were all found in “translation”. Genes encoding *RPL9*, *RPS7*, *RPS9* etc. were found in “ribosome”. *RPL9*, *RPL11*, *RPS7* and *RPS9* etc. were found in “structural constituent of ribosomes” (Additional file 4: Table S10). Structural component of ribosome, translation and ribosome were highly enriched among the GO terms ($P < 0.05$) (Fig. 7b and Additional file 4: Table S10).

Using KEGG annotation, the DEGs were found most in environmental information processing and metabolism, among which KEGG subclasses translation and amino acid metabolism (Fig. 8a, purple histogram) were predominant, with S gene numbers of 83 and 52, respectively (Fig. 8a). The DEGs were successfully annotated as members of 242 pathways (Additional file 4: Table S11). The ribosome pathway of the KEGG subclass translation was most significantly enriched, with the S gene number being 58 ($P < 0.05$) (Fig. 8b and Additional file 4: Table S12). *RPS7*, *RPS9*, *RPL9*, *RPL11* and 40S ribosomal protein S10b (*RPS10b*), ribosome biogenesis, RNA binding, metal ion binding, etc. were found in the ribosome pathway (Additional file 4: Table S11). It was concluded from GO and KEGG enrichment analysis that NNM might detrimentally affect the structural constituent of ribosomes or aminoacyl-tRNA synthetases, resulting in inhibition of the translation process.

Validation of RNA-Seq data by qPCR for selected genes

To validate the RNA-Seq results, ten DEGs, that had been randomly selected from RNA-Seq data, were verified using qPCR. Their expression trends were found to be similar to those obtained by RNA-Seq, indicating that the RNA-Seq data reliably reflected the gene expression levels (Additional file 3: Figure S3).

Effects of NNM on related gene expression levels involved in translation of *D. segeticola* comparing with CHX

We selected six DEGs of *RPS7*, *RPS9*, *RPS10b*, *RPL9*, *RPL11* and *TrpRS*, related to translation, based on the GO and KEGG enrichment analysis. The expression levels of *RPS7*, *RPS9*, *RPS10b*, *RPL9*, *RPL11* and *TrpRS* of *D. segeticola* were studied using qPCR to analyze the gene expression trends of the fungus in response to NNM and CHX at the dosages of EC_{10}, EC_{30} or EC_{50} and the treatment times of 1, 6 or 12 h.

After NNM treatment for 1 h, the expression levels of the six genes were significantly down-regulated (relative to the control) at the dosages of EC_{10}, EC_{30} and EC_{50} following 1 h treatment. Down-regulation trends for NNM treatment for 1 h indicated that exposure to NNM resulted in no significant differences among the three dosages (Fig. 9a to f, left). After treatment with NNM for 6 h, the expression levels of the six genes were down-regulated (relative to the control) at the concentration of EC_{10}, especially genes *RPS7*, *RPS9* and *RPL9* (Fig. 9a to f, left). The responses of gene expression at concentrations EC_{10} and EC_{50} were similar (Fig. 9a to f, left). On the other hand, the expression levels of *RPS7*, *RPS9*, *RPS10b*, *RPL9* and *RPL11* were significantly up-regulated at the dosage of EC_{30} (Fig. 9a to e, left). The results indicated that there was a compensatory or feedback regulation at the intermediate concentration. However, *TrpRS* has a different trend with significantly down-regulated at the dosage of EC_{30} (Fig. 9f, left). After 12 h NNM treatment, the expression levels of *RPS7*, *RPS9*, *RPS10b*, *RPL9* and *RPL11* were significantly up-regulated at the concentration of EC_{10}, with the expression level being slightly up-regulated, though not significantly so, at the concentrations of EC_{30} or EC_{50} (Fig. 9a to e, left). As the dosage increased, the up-regulated trends were less clear cut (Fig. 9a to e, left), with *RPS10b* even showing slightly down-regulation at EC_{50} following 12 h treatment (Fig. 9c, left). Nevertheless, the expression levels of *TrpRS* were all up-regulated. Along with the dosage being increased, the up-regulated trends represented more distinctly, especially at the dosage of EC_{50} (Fig. 9f, left).

As translation extension inhibitor, CHX treatment has different trends comparing NNM treatment. After 1 h treatment, *RPS7*, *RPS10b* and *RPL9* presented down-regulated at the dosages of EC_{10} and EC_{30} and slightly up-regulated at the dosage of EC_{50} (Fig. 9a, c and d, right). The *RPS9*, *RPL11* and *TrpRS* had no similar rule but presented up-regulated at most dosages (Fig. 9b, e and f, right). After 6 h treatment, *RPS9*, *RPS10b*, *RPL9* and *TrpRS* all presented up-regulated significantly. However, they presented down-regulated significantly at the dosages of EC_{30} and EC_{50} (Fig. 9b to d and f, right). *RPS7* presented down-regulated but *RPL11* up-regulated (Fig. 9a and e, right). After 12 h treatment, *RPS9*, *RPS10b*, *RPL9* and *TrpRS* presented down-regulated but *RPS7* and *RPL11* up-regulated at the dosage of EC_{10}. These six DEGs were all up-regulated at dosage of EC_{30} and down-regulated at the dosage of EC_{50} (Fig. 9a to f, right).

Molecular docking of NNM and proteins involved in translation

To study the potential targets of NNM, six proteins, namely TrpRS, RPS7, RPS9, RPS10b, RPL9 and RPL11, were selected for molecular docking studies with NNM. The DNA sequences were translated into protein sequences and run by BLAST in UniProt. Unfortunately, there are no crystal structures available

for any of the six protein sequences. We then used SWISS-MODEL to perform the homology modeling study, and the templates and identities of each protein are shown in Additional file 4: Table S13.

The homology models of the six proteins were obtained, and the proposed binding mode was analyzed for each protein-NNM combination, according to their interactions, the docking score and the binding free energy (Table 1). Among these proteins, TrpRS was the most potent target with a binding free energy of -101.55 kcal/mol. NNM could form a series of hydrogen bonds with Gly65, Arg66, Gly67, Gly76, His77, Thr100, Ser217, Asp219 and Lys256 (Fig. 10a). The potent binding pockets of these models were predicted using fpocket, and RPS7, RPS9, RPS10b, RPL9 and RPL11 were all found not to possess binding pockets. TrpRS protein was found to exhibit two highly potent binding pockets (Fig. 10b, red and green). NNM docked into these two pockets. It was found that the amino acid sequence of TrpRS had a key amino acid deletion near one binding pocket (Fig. 10c, red segment), compared with the template. When NNM docked to the template protein, it bound tightly, making it the most likely target for NNM binding.

Table 1 The docking score and binding free energy (kcal/mol) of Ningnanmycin (NNM) with six homology models.

Gene ID	Protein Name	Docking Score	Binding free energy (kcal/mol)
GZSQ4008008	Tryptophanyl-tRNA synthetase	-9.65	-101.55
GZSQ4005420	40S ribosomal protein S10-B	-4.32	-31.58
GZSQ4003254	60S ribosomal protein L11	-6.58	-32.34
GZSQ4008719	40S ribosomal protein S9	-5.32	-19.42
GZSQ4002876	40S ribosomal protein S7	-7.13	-40.20
GZSQ4007725	60S ribosomal protein-like protein L9	-6.33	-45.49

Discussion

Tea leaf spot, caused by *D. segeticola*, is one of the most important diseases of the tea crop, resulting in losses in tea production and tea quality [2] .Because of the absence of any effective biofungicide or similar environmentally protective measure, the prevention and control of tea leaf spot, caused by *D. segeticola*, is an important problem in the major tea-growing areas [2]. NNM, a biogenic antimicrobial, has already demonstrated a wide range of activity *in vitro* against many crop diseases [10–13].

In this study, we first determined that NNM inhibited the growth of hyphae of *D. segeticola* (Fig. 1 and Additional file 4: Table S1). Then, we observed that this inhibition was associated with morphological changes to the hyphae in response to NNM, such as inflated hyphae, appearance of granulations and decreased cytoplasmic density, but not in the obvious fungicidal changes concerning integrity of the cell

wall, sterol content or osmotic pressure (Fig. 2 and Fig. 5). These results indicated that NNM may not function as a classical fungicide, such as the triazole or strobilurin fungicides, which work by inhibiting the biosynthesis of sterols or inhibiting energy synthesis [17, 18].

As a consequence, the mode of action of NNM against *D. segeticola* would be of great interest and potential significance. The work would be helpful in developing a fungicide, with high antifungal activity, to manage tea leaf spot caused by *D. segeticola*. In our study, the mophological change also provided some information as to how NNM functioned. For instance, NNM was shown to be able to affect the formation and distribution of nuclei (Fig. 3), the development of septa (Fig. 4), the formation and development of organelles and the content of lipid bodies (Fig. 6). So, we speculated that NNM could possess the bioactivity of inhibiting fungal biosynthesis. To focus more clearly on the mode of action, we evaluated the response of hyphal gene expression to NNM, by identifying DEGs involved in the NNM/control comparison and associated with biosynthesis. Comparing the analyses by GO and KEGG, structural constituents of ribosomes were shown to be significantly enriched at MF, with the S gene number being 56 (Fig. 7), whereas 58 genes were significantly enriched in the ribosome pathway (Fig. 8). In addition, 54 genes were significantly enriched in translation at BP, and 38 genes were significantly enriched with ribosomes at CC (Fig. 7). Furthermore, all the above genes belong to the KEGG subclass of translation. Combining the morphological analysis with GO and KEGG enrichment analysis, we speculated that NNM might affect translation.

The process of translation can be divided into four stages, namely initiation, elongation, termination and recycling. These stages were related to some genes of eukaryotic translation initiation factors, the structural constituents of small (40S) and large (60S) ribosomal subunits, aminoacyl-tRNA synthetases, amino acid synthesis, etc. Aminoacyl-tRNA synthetases are among the leading targets for the development of antibiotics [19]. TrpRS belongs to the aminoacyl-tRNA synthetases that play a pivotal role in protein synthesis and are essential for cell growth and survival [19]. Ribosomes are also known as a major target for small molecule inhibitors. For example, CHX is known as a small molecule inhibitor, targeting the eukaryotic ribosome [20]. Genes *RPS7*, *RPS9* and *RPS10b* encode proteins for the small ribosomal subunit that binds mRNAs, translating the encoded mRNA message by selecting cognate aminoacyl-tRNA molecules [21]. Proteins encoded by *RPL9* and *RPL11* belong to the large ribosomal subunit, containing the ribosomal catalytic site. This is termed the peptidyl transferase center, which catalyzes the formation of peptide bonds, thereby polymerizing the amino acids, delivered by tRNAs, into a polypeptide chain [21]. The above six genes are all related to the process of eukaryotic translation. In this study, qPCR assays indicated that these genes were up-regulated or down-regulated by NNM, with the effect of regulation being influenced by the dosage of NNM and treatment time. There were different trends after NNM treatment for 1, 6 and 12 h (Fig. 9). The results indicated that the expression of the small ribosomal subunit, the large ribosomal subunit and TrpRS were regulated by NNM at the mRNA expression level. Through CHX being set as a control agent for inhibition of ribosomes, we found that CHX and NNM can regulate expression of *TrpRS*, *RPS7*, *RPS9*, *RPS10b*, *RPL9* and *RPL11* at various dosages and under different treatment periods [22]. Nevertheless, there is also some difference between NNM and CHX treatments. As a consequence, we considered that NNM should be regarded as a TrpRS-

related inhibitor of translation. Based on this, we completed the homology modeling between NNM and the six proteins proposed. Among these proteins, TrpRS was the most potent target with a binding free energy of -101.55 kcal/mol. And the amino acid sequence of the TrpRS protein had a key amino acid deletion near the binding pocket, being the most likely target for NNM binding (Fig. 10c). Therefore, we considered that NNM affects translation, thus inhibiting the growth of the hyphae of *D. segeticola*, when the hyphae of *D. segeticola* were exposed to NNM. We constructed a possible model of NNM antifungal action mechanism based on all the above findings. NNM initially down-regulated the expression levels of the genes concerned, such as structural constituents of ribosomes and aminoacyl-tRNA synthases, involved in the translation process, after NNM had entered the fungal hyphal cell. More specifically, NNM targeted tryptophan tRNA synthetase, thereby inhibiting the translation process, so that the growth of fungal hyphal cells was subsequently inhibited, resulting in lowering of the density of the cytoplasm, reducing the integrity of the mitochondria and thickening the hyphal cell walls. Furthermore, the inhibition of translation might affect any protein-based biological processes, such as DNA replication and transcription.

Conclusions

NNM proved to exhibit antifungal activity *in vitro* toward *D. segeticola* in terms of inhibition of mycelial growth, and might function by inhibiting translation by binding to tryptophanyl-tRNA synthetase. NNM proved to be worthy of study to prevent and control tea leaf spot. In the future, we will further study the action mechanism of NNM against *D. segeticola*, using the method of site-directed mutagenesis, as well as evaluating the effect of NNM on *D. segeticola in vivo*.

Methods

Fungal isolates and source of NNM

D. segeticola was identified in our research group [7], and deposited in China General Microbiological Culture Collection Center, with the preservation number of fungus as CGMCC3.20152. NNM was kindly provided by Jiaren Chen, researcher at Chengdu Institute of Biology, Chinese Academy of Sciences (Chengdu, Sichuan Province, China). One unit (1 U) of NNM is equivalent to 2.15 μg of NNM.

Antifungal activity of NNM on *D. segeticola in vitro*

The antifungal activity of NNM was determined *in vitro* over six concentrations (0-3,000 U/mL) against *D. segeticola* by the mycelial growth rate method [23]. NNM was dissolved in sterilized distilled water before mixing with nine volumes of potato dextrose agar (PDA, Beijing Solarbio Science & Technology Co., Ltd., Beijing, China), and poured into 9-cm culture dishes to prepare the plate medium. Mycelium plugs (4 mm diameter) were cut from the leading edge of the 7-day-old culture medium, and were inoculated onto the center of the PDA plates (control and treatments, i.e., different NNM concentrations) containing cellulose acetate membrane, with a sterilized inoculation needle. The dishes were incubated at 25°C for 7 days.

The inhibition rate (%) of NNM against *D. segeticola* growth was calculated through the following equation:

I = [(C - T)/(C - 0.4)] * 100 (Eqn. 1)

where I represents the inhibition rate, C represents the diameter (mm) of the fungus colony (after substraction of the plug diameter) on control (0 U/mL NNM) PDA and T represents the diameter (mm) of the fungus colony (after subtraction of the plug diameter) on PDA containing NNM.

After that, the mycelium together with cellulose acetate membrane was dried to constant weight at 60°C. The effect of NNM concentration on dry weight of *D. segeticola* was calculated through the following equation:

I = [(S - A)/S] * 100 (Eqn. 2)

where I represents the inhibition rate (%) and S (g) and A (g) are the mean dry weights of the control mycelium and treatment mycelium, respectively.

Effect of NNM on mycelial morphology and ultrastructure of *D. segeticola*

Mycelial plugs (4 mm diameter) from the leading edge of a 7-day-old colony of *D. segeticola* were transferred to 250-mL conical flasks, containing 90 mL potato dextrose broth (PDB, Solarbio Science & Technology Co., Ltd., Beijing, China), in a shaking incubator at 180 rpm, 25°C for 60 h in darkness. After that, NNM in 10 mL sterile ddH_2O containing NNM was added to 90 mL PDB to achieve final concentrations representing EC_{10}, EC_{30} or EC_{50}, respectively) as the treatment or 10 mL sterile water without NNM to 90 mL PDB as the control. We collected the mycelia from PDB after 1 h and 14 h incubation for microscopic examination of mycelial morphology. Sample observation was carried out by optical microscopy (BX53, Olympus, Tokyo, Japan) [24], SEM (U8010, Hitachi, Tokyo, Japan) [24] and TEM (Tecnai G2 20 S-Twin, FEI, Hillsboro, OR, USA) [25], with three replications of each treatment.

Effect of NNM on cell nucleus andseptum structure of *D. segeticola*

The sample preparation for fluorescence microscopy was the same as that for mycelial morphology observations of *D. segeticola*. We collected mycelium from PDB plus/minus NNM shake cultures after 1, 12 and 24 h treatment as samples for fluorescence staining. In order to observe cell nuclei and septa, mycelia were washed twice using 0.1M phosphate-buffered saline (PBS, pH=7.4), and mycelia were then stained, using 1 μg/mL 4', 6-diamidino-2-phenylindole (DAPI, Biofroxx, Guangzhou Saiguo Biotech Co., Ltd, Guangzhou, China) in 200 μL volumes of mycelial suspension for 30 min in the dark [26]. To observe septa, we stained the mycelia with 200 μL Calcofluor White (CFW, Sigma-Aldrich, Shanghai, China) at 1 μg/mL for 30 s in the dark [26]. After being washed three times with PBS, the cell nuclei and septa of the mycelia were observed by fluorescence microscopy (U-HGLGPS for BX53, Olympus).

RNA isolation, library construction and sequencing

A total of six RNA samples from control and treatment groups (Three biological replicates each group) were extracted using TRIzol reagent (Invitrogen, Carlsbad, CA, USA), following the manufacturer's procedure. The total RNA quantity and purity were determined using a Bioanalyzer 2100 and the RNA 1000 Nano LabChip Kit (Agilent, Palo Alto, CA, USA), with RNA Integrity Number (RIN) >7.0. Poly(A)-RNA was purified from total RNA (5 μg), using poly-T oligo-attached magnetic beads (dynabeads Oligo (dT),Thermo Fisher, Waltham, MA, USA), with two rounds of purification. Following purification, the mRNAs were fragmented into small pieces using NEBNext® Magnesium RNA Fragmentation Module (NEB, Ipswich, MA, USA). Then, the cleaved RNA fragments were reverse-transcribed to create the final cDNA library in accordance with the protocol for the TruSeq® RNA-Seq Sample Preparation kit (Illumina, San Diego, CA, USA), with the average insert size for the paired-end libraries being 300 bp (±50 bp). Sequencing was then carried out on an Illumina HiSeq 4000 (Lianchuan Biological Technology Co., Ltd., Hangzhou, China) to yield 2 × 150 bp paired-end raw reads, following the manufacturer's recommended protocol.

De novo assembly, annotation and identification of DEGs

The sequenced raw reads were subjected to a quality check, using RSeQC (v2.4) (https://github.com/MonashBioinformaticsPlatform/RSeQC) in the R package [27]. The adapter sequences were removed from the raw reads. Reads with a ratio of ambiguous N nucleotides greater than 5% and those with low-quality sequences (quality score of less than 20) were also removed. The filtered clean reads were then mapped to the *D. segeticola* reference genome, using the HISAT (v2.1.0) (http://daehwankimlab.github.io/hisat2/) algorithm package [28], which initially removes a portion of the reads based on quality information accompanying each read and then maps the reads to the reference genome, *D. bellidis*. HISAT allows multiple alignments per read (up to 20 by default) and a maximum of two mismatches, when mapping the reads aligned to the reference genome. HISAT builds up a database of potential splice junctions and confirms these by comparing the previously unmapped reads against the database of putative junctions. The mapped reads of each sample were assembled using StringTie (v1.3.0) (https://ccb.jhu.edu/software/stringtie/history.shtml) [29]. Then, all transcriptomes from the samples were merged to construct a comprehensive transcriptome, using Perl scripts. After the final transcriptome was generated, StringTie and edgeR (https://bioconductor.org/packages/release/bioc/html/edgeR.html) were used to estimate the expression levels of all transcripts. StringTie was used to determine the expression level for mRNAs by calculating FPKM [30]. The differentially expressed mRNAs and genes were selected with |log2(fold change)| > 1 or |log2(fold change)| < -1, and with statistical significance ($P < 0.05$), using the R package (v3.2.5) (https://www.r-project.org/).

GO and KEGG enrichment analysis

GO term enrichment was analysed using the Gene Ontology Enrichment Analysis Software Toolkit (http://geneontology.org) [31] and statistical enrichment was considered when $P < 0.05$. The Kyoto

Encyclopedia of Genes and Genomes (KEGG) analysis was performed by the Database for Annotation (http://www.kegg.jp/kegg) [32].

Gene expression validation by quantitative real time Polymerase Chain Reaction (qPCR)

For qPCR, 1 μg of the total RNA used in the previous RNA-Seq library construction was used for cDNA synthesis, which was performed using TUREscript 1st Stand cDNA Synthesis Kit (Aidlab Biotech Co., Ltd., Beijing, China). The qPCR was performed using 2×SYBR® Green Premixed (DBI®Bioscience, Ludwigshafen, Germany). The actin gene of *Didymella* was used as the internal control. The primers were designed using Primer3web (v4.1.0) (http://primer3.ut.ee/) and synthesized by TsingKe Biotech Co., Ltd (Beijing, China). The primer sequences are listed in Additional file 4: Table S14. The relative expression levels were calculated using the $2^{-\Delta\Delta CT}$ method [33].

Effects of NNM on the expression of genes involved in the translation of *D. segeticola*

We investigated the expression levels of *D. segeticola* genes involved in the ribosome pathway and the GO term of translation in samples with or without NNM treatment at the concentration of 47.23 U/mL (EC_{10}), 341.98 U/mL (EC_{30}) or 1287.54 U/mL (EC_{50}), using qPCR. Samples treated with cycloheximide (CHX) (99.86% purity, MCE, Shanghai, China) at three concentrations of EC_{10}, EC_{30} and EC_{50} values were used as translation elongation inhibitor [34]. First, CHX was dissolved in 200 μL dimethyl sulfoxide (DMSO) (Beijing Solarbio Science & Technology Co., Ltd., Beijing, China) to prepare the stock solution. Then, 10 mL sterilized double-distilled H_2O (ddH_2O), containing 0.1% (v/v) Tween-20 (Sangon Biotech. Co., Ltd., Shanghai, China), were mixed with different amounts of the NNM stock solutions, and the solutions were further mixed with molten 90 mL PDB to obtain final concentrations of 0, EC_{10}, EC_{30} or EC_{50} NNM, respectively. After 1, 6 and 12 h of continuous shaking under the same conditions as described earlier, mycelial samples from each treatment were centrifuged and washed twice with PBS. Total RNA extraction, cDNA synthesis and qPCR analysis were performed as described previously. The DEGs and primers involved in the translation process are listed in Additional file 4: Table S15.

Molecular docking of NNM and proteins involved in translation

The DNA sequences identified as DEGs were translated into protein sequences and screened for in the UniProt database, with BLAST. The target sequence was searched with BLAST [35] against the primary amino acid sequence contained in the SWISS-MODEL template library [36]. Models were built, based on the target-template alignment, using ProMod3 (https://openstructure.org/promod3/3.1/) [37]. The homology models of the proteins were obtained, and the potent binding pockets of these models were predicted using fpocket (https://bio.tools/fpocket) [38]. NNM was docked into these pockets with AutoDock vina (https://bio.tools/AutoDock_Vina) [39] and the binding free energy was calculated using the MM/PBSA method [40].

Statistical analyses

The data were presented as the mean values ± standard error (SE) of three replicates. Data analysis of variance using Duncan's multiple range tests of SPSS (v19.0) (IBM, Armonk, NY, USA) and performing the least significant difference at 0.05 levels using lowercase letters.

Abbreviations

D. segeticola: *Didymella segeticola*; *D. bellidis*: *Didymella bellidis*; FPKM: Fragments per kilobase of exon model per million mapped reads; GO: Gene Ontology; KEGG: Kyoto Encyclopedia of Genes and Genomes; qPCR: quantitative real time polymerase chain reaction; NNM: Ningnanmycin; CHX: Cycloheximide; DMSO: Dimethyl sulfoxide; ddH_2O: double-distilled H_2O; SE: Standard error; EC_{50}: Half-maximal effective concentration; DAPI: 4',6-diamidino-2-phenylindole; CFW: Calcofluor White; DEGs: Differentially expressed genes; RIN: RNA integrity number; BP: Biological Process; MF: Molecular Function; CC: Cellular Component; *RPS7*: 40S ribosomal protein S7; *RPS9*: 40S ribosomal protein S9; *RPS10b*: 40S ribosomal protein S10b; *RPL9*: 60S ribosomal protein L9; RPL11: 60S ribosomal protein L11; *TrpRS*: Tryptophanyl-tRNA synthetase; PDA: Potato dextrose agar; PDB: Potato dextrose broth; PBS: Phosphate-buffered saline

Declarations

Acknowledgments

We thank Hangzhou Lianchuan Biological Technology Co., Ltd. for helping us with transcriptome and experiments and data analysis. And we would like to Gefei Hao for molecular docking data analysis.

Author's contributions

DL performed the experiment of antifungal bioactivity, transcriptome and performed the data analysis in this work. QY, XW, SJ, DD and XW helped the data analysis. DW designed the experiments and wrote the manuscript and. ZC designed the experiments, conducted the whole study and edited the article. All authors have read and degreed to published version of the manuscript.

Funding

This work was supported by National Key Research Development Program of China (2017YFD0200308) and its Post-subsidy project (2018-5262), the National Natural Science Foundation of China (No. 21977023, No.31860515), the China Agriculture Research System (CARS-23-D09).

Availability of data and materials

RNA-sequencing raw data of *Didymella segeticola* treated with Ningnanmycin has been submitted to NCBI Sequence Read Archive database (SRA) under accession number PRJNA579490 (https://www.ncbi.nlm.nih.gov/bioproject/?term=PRJNA579490). The whole genome of *D. segeticola* can be download in NCBI SRA database under accession number PRJNA516041 (https://www.ncbi.nlm.nih.gov/bioproject/?term=PRJNA516041). The raw data of transcriptome analysis

of *D. segeticola* cultured on PDA medium and PDA-matcha mixed medium can be download in NCBI SRA database under accession number PRJNA648680 (https://www.ncbi.nlm.nih.gov/bioproject/?term=PRJNA648680). The raw data of RNA-Seq of tea plant (*Camellia sinensis*) leaves infected by *D. segeticola* can be download in NCBI SRA database under accession number PRJNA528172 (https://www.ncbi.nlm.nih.gov/bioproject/?term=PRJNA528172). The raw data of small RNAs sequencing of tea plant infected with *D. segeticola* can be download in NCBI SRA database under accession number PRJNA534364 (https://www.ncbi.nlm.nih.gov/bioproject/?term=PRJNA534364).

Ethics approval and consent to participate

Not Applicable.

Consent for publication

Not Applicable.

Competing interests

The authors declare that they have no competing interests.

Author details

[1]Key Laboratory of Green Pesticide and Agricultural Bioengineering, Ministry of Education, Guizhou University, Guiyang Guizhou 550025, China. [2]College of Agriculture, Guizhou University, Guiyang 550025, China. [3]College of Forestry, Guizhou University, Guiyang Guizhou 550025, China

References

1. Li DX, Bao XT, Wang Y, Ren YF, Song BA, Chen Z. First report of *Lasiodiplodia theobromae* causing leaf spot on tea plant in Guizhou Province of China. Plant Dis. 2019;103:374.
2. Zhao XZ, Wang Y, Li DX, Ren YF, Chen Z. Morphological characterization and phylogenetic analysis of the pathogen *Phoma segeticolacamelliae* causing a new tea disease (in Chinese). Acta Phytopathologica Sinica. 2018;48:556-559.
3. Bao XT, Dharmasena DSP, Li DX, Wang X, Jiang SL, Ren YF, et al. First report of *Epicoccum sorghinum* causing leaf spot on tea in China. Plant Dis. 2019;103:3282.
4. Wang X, Yin QX, Jiang SL, Wu X, Wang DL, Song BA, et al. First report of *Didymella bellidis* causing tea leaf spot in China. Plant Dis. 2020;104:1254.
5. Zhou LX, Xu WX. First Report of *Alternaria alternata* causing leaf spots of tea (*Camellia sinensis*) in China. Plant Dis. 2014;98:697.
6. Liu Z, Liu T, Chen D, Hou JM. First report of *Curvularia lunata* causing leaf spots on Partridge tea [*Mallotus oblongifolius* (Miq.) Mûll. Arg.] in China. J Plant Pathol. 2019;101:439.

7. Zhao XZ, Chen Z, Yu L, Hu DY, Song BA. Investigating the antifungal activity and mechanism of a microbial pesticide Shenqinmycin against, *Phoma* Pestic Biochem Phys. 2018;147:46-50.
8. Chen Q, Hou LW, Duan WJ, Crous PW, Cai L. *Didymellaceae* Stud Mycol. 2017;87:105-159.
9. Xiang GX, Hu HZ, Chen JR, Chen WX, Wu LS. A new agricultural antibiotic-Ningnanmycin (in Chinese). Acta Microbiologica Sinica. 1995;35:368-374.
10. Deng GB, Wang B, Hu HZ, Chen JR, Yu MQ. Biological activity of Ningnanmycin on tobacco mosaic virus (in Chinese). Chin J Appl Environ Biol. 2004;10:695-698.
11. Hu HZ, Zhao XY. Studies on application of Ningnanmycin to mosaic diseases of tobacco (in Chinese). Chin J Appl Environ Biol. 1998;4:390-395.
12. Liu Z, Du LF, Zhang NH, Deng GB, Yu MQ, Chen JR, et al. Induced expression of acidic pathogenesis-related proteins in tobacco by Ningnanmycin (in Chinese). Chin J Appl Environ Biol. 2005;11:549-553.
13. Gao D, Wang DM, Chen K, Huang MX, Xie X, Li XY. Activation of biochemical factors in CMV-infected tobacco by Ningnanmycin. Pestic Biochem Physio. 2019;156:116-122.
14. Li XY, Hao GF, Wang QM, Chen Z, Ding Y, Yu L, et al. Ningnanmycin inhibits tobacco mosaic virus virulence by binding directly to its coat protein discs. Oncotarget. 2017;8:82446-82458.
15. Ren YF, Li DX, Zhao XZ, Wang Y, Bao XT, Wang X, et al. Whole genome sequences of the tea leaf spot pathogen *Didymella segeticola*. Phytopathology. 2019;109:1676-1678.
16. Yang R, Jiang SL, Li DX, Yin QX, Wu X, Wang Y, et al. Integrated mRNA and small RNA sequencing for analyzing leaf spot pathogen *Didymella segeticola* and its host, tea (*Camellia sinensis*), during infection. Mol Plant Microbe In. 2020; doi: 1094/MPMI-07-20-0207-A.
17. Bertelsen JR, Neergaard ED, Smedegaard–Petersen V. Fungicidal effects of azoxystrobin and epoxiconazole on phyllosphere fungi, senescence and yield of winter wheat. Plant Pathol. 2001;50:190-205.
18. Ziogas BN, Oesterhelt G, Masner P, Steel CC, Furter R. Fenpropimorph: a three site inhibitor of ergosterol biosynthesis in *Nectria haematococcacucurbitae*. Pestic Biochem Physiol. 1991;39:74-83.
19. Zhao YX, Meng QQ, Bai LQ, Zhou HC. *In silico* discovery of aminoacyl-tRNA synthetase inhibitors. Int J Mol Sci. 2014;15:1358-1373.
20. Loubresse NG, Prokhorova I, Holtkamp W, Rodnina MV, Yusupova G, Yusupov M. Structural basis for the inhibition of the eukaryotic ribosome. Nature. 2014;513:517-522.
21. Ben-Shem A, Loubresse NG, Melnikov S, Jenner L, Yusupova G, Yusupov M. The structure of the eukaryotic ribosome at 3.0 Å resolution. Science. 2011;334:1524-1529.
22. Santos DA, Shi L, Tu BP, Weissman JS. Cycloheximide can distort measurements of mRNA levels and translation efficiency. Nucleic Acids Res. 2019;10:4974-4985.
23. Chattapadhyay TK, Dureja P. Antifungal activity of 4-methyl-6-alkyl-2H-pyran-2-ones. J Agric Food Chem. 2006;54:2129-2133.

24. Zheng L, Zhao J, Liang XF, Zhan GM, Jiang SC, Kang ZS. Identification of a novel *Alternaria alternata* strain able to hyperparasitize *Puccinia striiformis* sp. *tritici*, the causal agent of wheat stripe rust. Front Microbiol. 2017;8:71.
25. Zhang J, Han RY, Ye HC, Zhou Y, Zhang ZK, Yuan EL, et al. Effect of PAB on biochemical and physiologic characteristics in *Colletotrichum gloeosporioides*. Pestic Biochem Phys. 2017;147:75-82.
26. Chen YL, Mao XW, Wang JX, Wu LY, Zhou MG, Hou YP. Activity of the dinitroaniline fungicide fluazinam against *Bipolaris maydis*. Pestic Biochem Phys. 2018;148:8-15.
27. Wang LG, Wang SQ, Li W. RSeQC: Quality control of RNA-seq experiments. Bioinformatics. 2012;28:2184-2185.
28. Kim D, Langmead B, Salzberg SL. HISAT: a fast spliced aligner with low memory requirements. Nat Methods. 2015;12:357-360.
29. Pertea M, Pertea GM, Antonescu CM, Chang TC, Mendell JT, Salzberg SL. StringTie enables improved reconstruction of a transcriptome from RNA-seq reads. Nat Biotechnol. 2015;33:290-295.
30. Trapnell C, Williams BA, Pertea G, Mortazavi A, Kwan G, Van Baren MJ, et al. Transcript assembly and quantification by RNA-Seq reveals unannotated transcripts and isoform switching during cell differentiation. Nat Biotechnol. 2010;28:511-515.
31. Young MD, Wakefield MJ, Smyth GK, Oshlack A. Gene ontology analysis for RNA-seq: accounting for selection bias. Genome Biol. 2010;11:R14.
32. Kanehisa M, Araki M, Goto S, Hattori M, Hirakawa M, Itoh M, et al. KEGG for linking genomes to life and the environment. Nucleic Acids Res. 2008;36:D480-D484.
33. Schmittgen TD, Livak KJ. Analyzing real-time PCR data by the comparative C(T) method. Nat Protoc. 2008;3:1101-1108.
34. Schneider-Poetsch T, Ju JH, Eyler DE, Dang YJ, Bhat S, Merrick WC, et al. Inhibition of eukaryotic translation elongation by cycloheximide and lactimidomycin. Nat Chem Biol. 2010;6:209-217.
35. Camacho C, Coulouris G, Avagyan V, Ma N, Papadopoulos J, Bealer K, et al. BLAST+: architecture and applications. BMC Bioinformatics. 2009;10:421-430.
36. Bienert S, Waterhouse A, de Beer TAP, Tauriello G, Studer G, Bordoli L, et al. The SWISS-MODEL Repository-new features and functionality. Nucleic Acids Res. 2017;45:D313-D319.
37. Waterhouse A, Bertoni M, Bienert S, Studer G, Tauriello G, Gumienny R, et al. SWISS-MODEL: homology modelling of protein structures and complexes. Nucleic Acids Res. 2018;46:W296-W303.
38. Schmidtke P, Bidon-Chanal A, Luque J, Barril X. MDpocket: open source cavity detection and characterization on molecular dynamics trajectories. Bioinformatics. 2011;27:3276-3285.
39. Trott O, Olson AJ. AutoDock Vina: improving the speed and accuracy of docking with a new scoring function, efficient optimization and multithreading. J Comput Chem. 2010;31:455-461.
40. Gnheden S, Ryde U. The MM/PBSA and MM/GBSA methods to estimate ligand-binding affinities. Expert Opin Drug Dis. 2015;10:449-461.

Supporting Information

Supporting information may be found in the online version of this article.

Additional file 1: Figure S1 The expressed level analysis of all genes. a. The boxplot of gene expression values. X-axis, detected sample names, Control_1_hr_1-Control_1_hr_3 indicated three biological replicates in the control group; Ningnanmycin_1_hr_1-Ningnanmycin_1_hr_3 indicated three biological replicates in the treatment group. Y-axis, the relative expression level was expressed as $\log_{10}$(FPKM+1) in gene expression value. b. The density of gene expression values in two groups (the control group on the top of sub-figure and the treatment group on the bottom of sub-figure).

Additional file 2: Figure S2 The volcano of all Differentially expressed genes (DEGs) by transcription sequencing. The DEGs were selected by $P < 0.05$ and |log2(fold change)|> 1. The X-axis shows the fold change in gene expression between control and treatment groups, and the Y-axis shows the statistical significance of the differences. Splashes represent different genes. Red splashes mean significantly up-regulated expressed genes. Blue splashes mean significantly down-regulated expressed genes. Gray splashes mean genes without significant different expression.

Additional file 3: Figure S3 Expression levels profile comparisons between the RNA-Seq and qPCR data. X-axis, detected gene names; Y-axis, the relative expression level was expressed as log2(fold change) in gene expression. *ABC transporter*, ATP-binding cassette transporter; *EPHX*, epoxide hydrolase; *MIB*, metal ion binding; *CAT*, catalase; *NADPH-ADH*, nadph-dependent medium chain alcohol dehydrogenase; *MPI*, mannose-6-phosphate isomerase; *HEBP*, heme binding protein; *NRPS*, non-ribosomal peptide synthetase; *CDH*, choline dehydrogenase.

Additional file 4: Table S1 Effect of Ningnanmycin (NNM) on mycelial growth rate and biomass (dry weight, g) of *Didymella segeticola*. **Table S2.** Summary of the transcriptome sequencing data from two treatment samples. **Table S3.** The statistics of mapped reads for *Didymella segeticola*. **Table S4.** The region distribution of the valid reads in transcription sequencing. **Table S5.** Summary of transcription sequencing genes. **Table S6.** Gene annotation of all expressed genes from two groups. **Table S7.** The distribution of gene expression value each sample. **Table S8.** The different interval distribution of gene expression values. **Table S9.** The differential expression gene for NNM treatment for 1 h from two treatment. **Table S10.** The GO enrichment analysis of DEGs for two treatment groups. **Table S11.** KEGG enrichment analysis of DEGs for two treatment groups. **Table S12.** KEGG classification of significantly DEGs. **Table S13.** The protein and homology modeling template information. **Table S14.** The genes and primers used for transcriptome sequencing validation by qPCR analysis. **Table S15.** The differentially expressed genes (NNM treatment vs control) and primers used in translation process of *Didymella segeticola*.

Figures

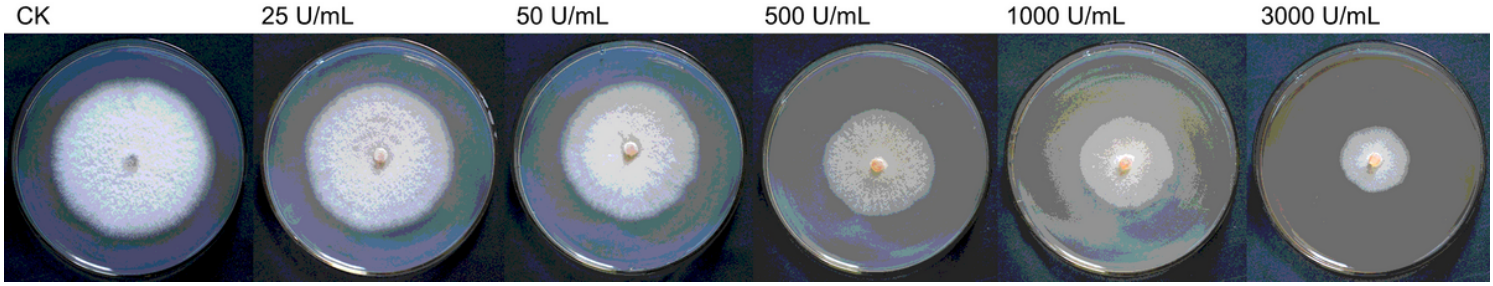

Figure 1

The colony morphology of Didymella segeticola on different dosages of Ningnanmycin (NNM). “CK” = control.

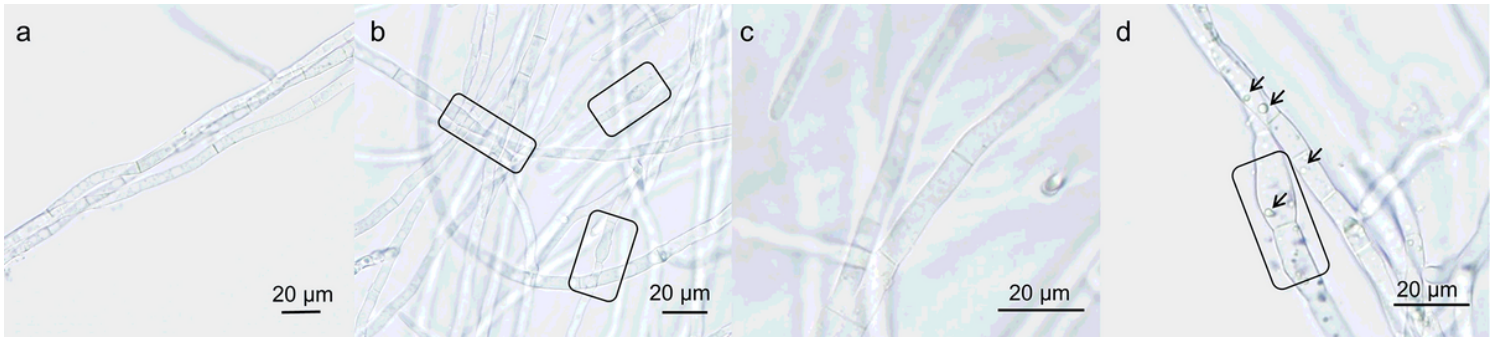

Figure 2

The hyphal morphology of Didymella segeticola exposure to half-maximal effective concentration (EC50) of Ningnanmycin (NNM). Control hyphae after 1 h (a); Hyphae treated for 1 h by NNM (b); Control hyphae after 14 h (c); Hyphal morphology treated for 14 h by NNM (d); Rectangles indicated the inflated hyphae. Arrows indicated the emerging granulations.

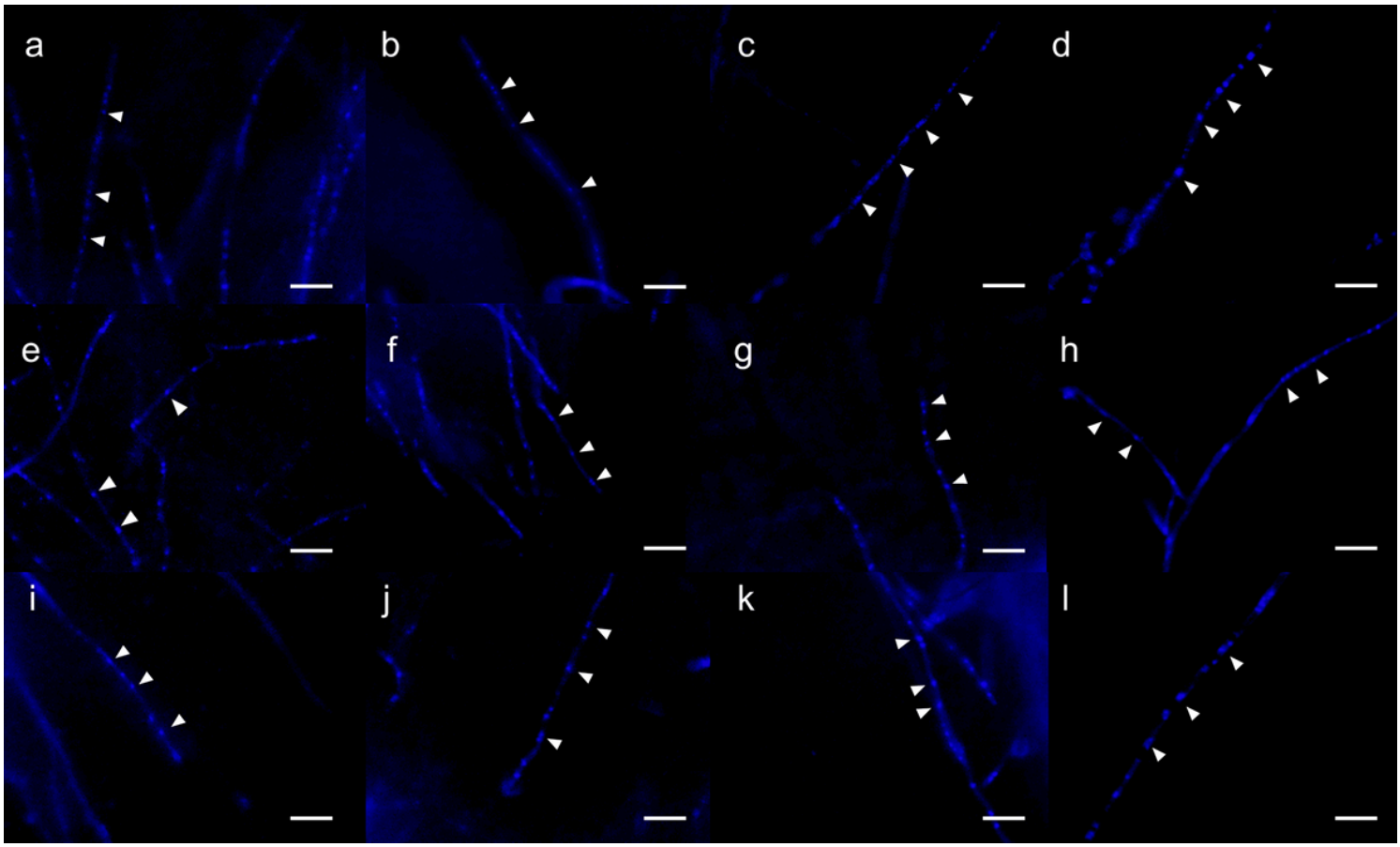

Figure 3

Effect of Ningnanmycin (NNM) on cellular nucleus distribution in hyphae stained with 4',6-diamidino-2-phenylindole (DAPI). Didymella segeticola was treated with NNM at the concentrations of 0 U/mL (a), EC10 (b), EC30 (c) or EC50 (d) for 1 h; D. segeticola treated with NNM at the concentrations of 0 U/mL (e), EC10 (f), EC30 (g) or EC50 (h) for 12 h; and D. segeticola treated with NNM at the concentrations of 0 U/mL (i), EC10 (j), EC30 (k) or EC50 (l) for 24 h. Scale bar = 50 μm. Arrows indicated the cell nuclei.

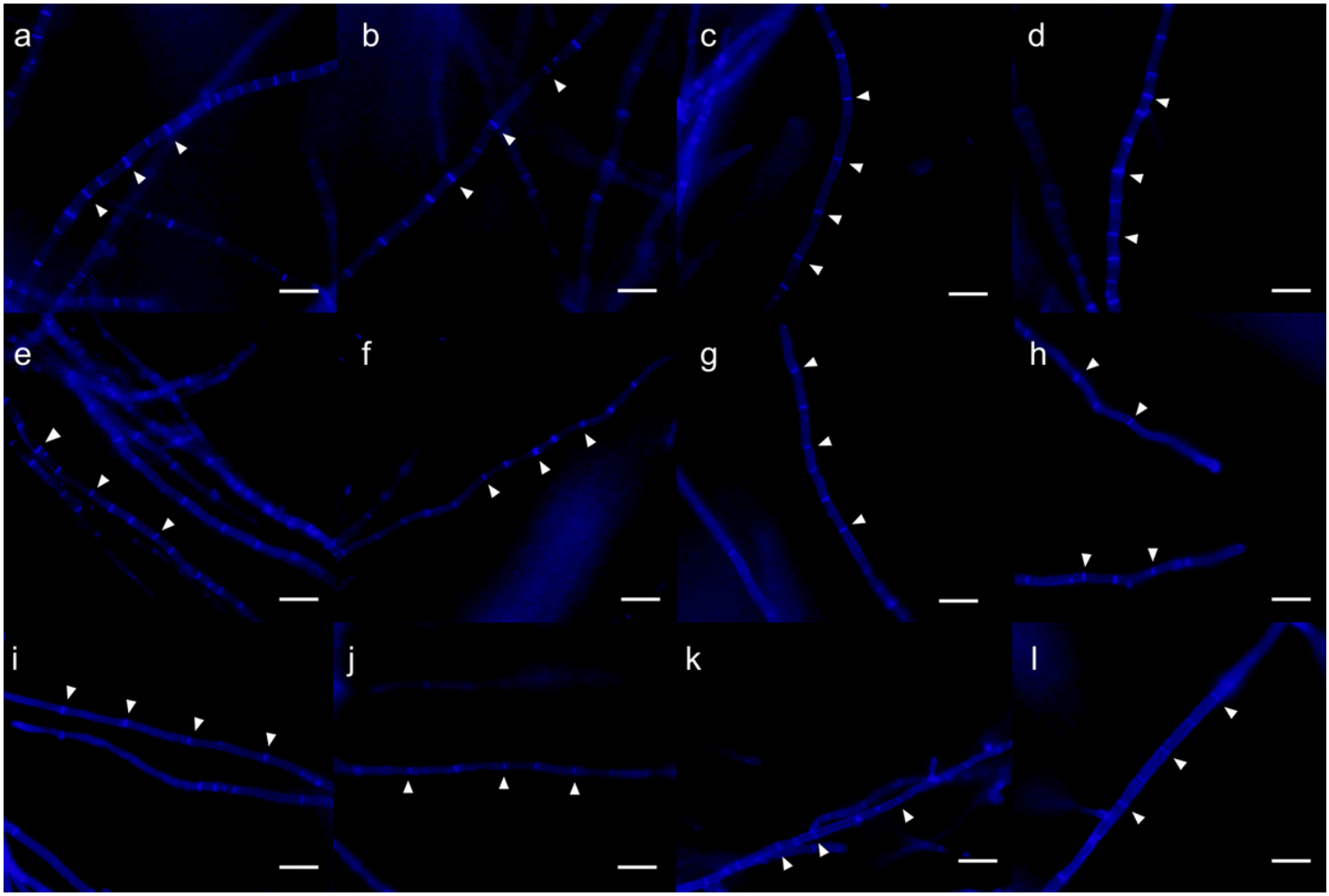

Figure 4

Effect of Ningnanmycin (NNM) on cellular septa in hyphae stained with Calcofluor White (CFW). Didymella segeticola treated with NNM with the concentrations of 0 U/mL (a), EC10 (b), EC30 (c) or EC50 (d) for 1 h; D. segeticola treated with NNM with the concentrations of 0 U/mL (e), EC10 (f), EC30 (g) or EC50 (h) for 12 h; D. segeticola treated with NNM with the concentrations of 0 U/mL (i), EC10 (j), EC30 (k) or EC50 (l) for 24 h. Scale bar = 50 μm. Arrows indicated the cell septa.

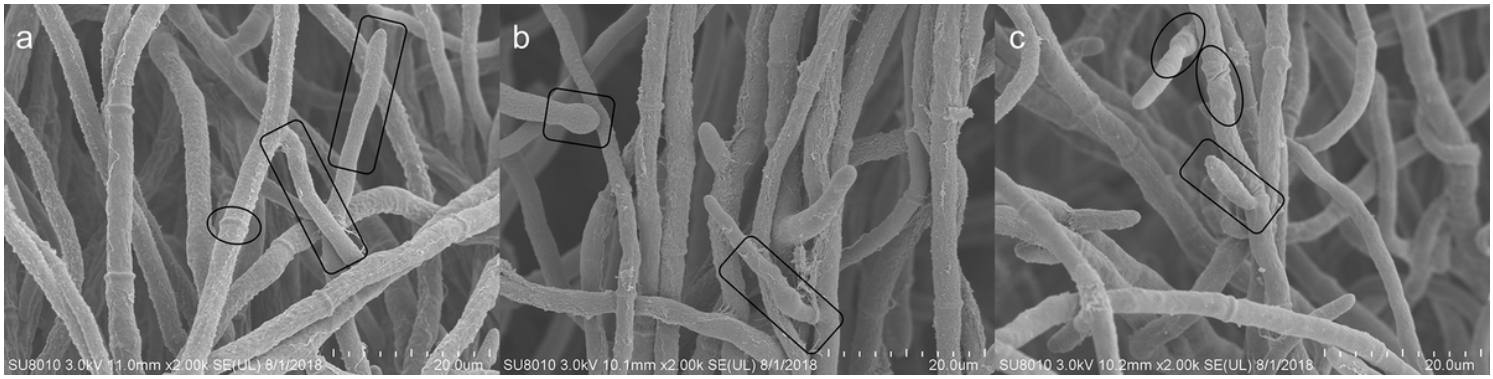

Figure 5

The hyphal morphology of Didymella segeticola observed under a scanning electron microscope. D. segeticola was induced by Ningnanmycin (NNM) at half-maximal effective concentration (EC50) for different treatment times. The morphology of control hyphae (a) and hyphae treated with NNM (b) after 1 h, and of control hyphae (c) and hyphae treated with NNM (d) after 14 h. Circles indicated cell septa, and rectangles indicated the morphology of hypha.

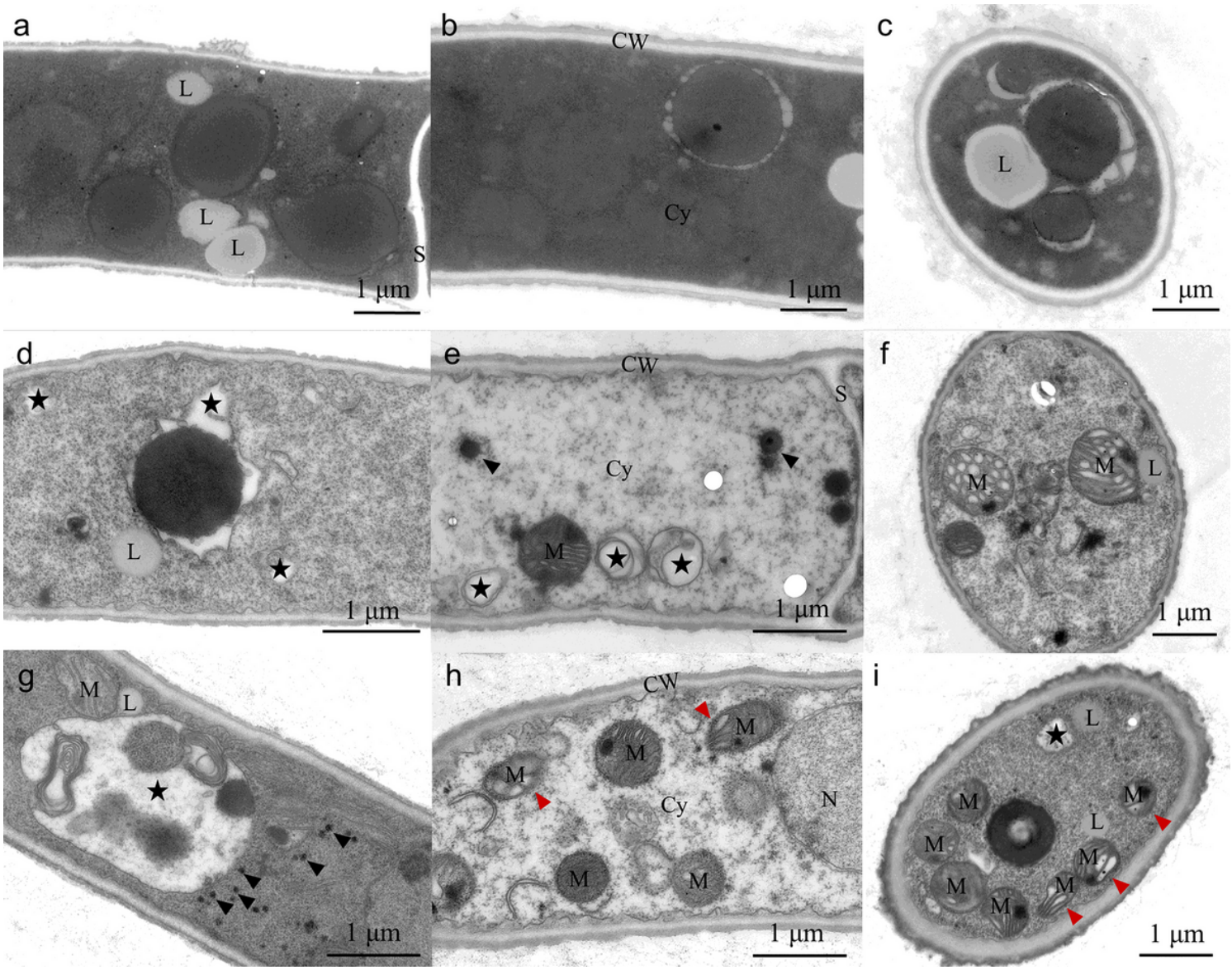

Figure 6

The hyphal morphology as seen under transmission electron microscopy. The hyphae of Didymella segeticola treated with Ningnanmycin (NNM) at 0 U/mL or half-maximal effective concentration (EC50) for different treatment times. Longitudinal section (a) and (b) and transverse section (c) of control hyphae treated for 0 h; Longitudinal section (d) and (e) and transverse section (f) of hyphae treated with NNM for 1 h; Longitudinal section (g) and (h) and transverse section (i) of hyphae treated with NNM for 14 h. Asterisks represented the cytoplasm appearing degraded, having developed empty spaces; M: mitochondrion; CW: cell wall; Cy: cytoplasm; N: nucleus; S: septum; L: lipid bodies. Black arrows indicated dense bodies; Red arrows indicated damaged mitochondria.

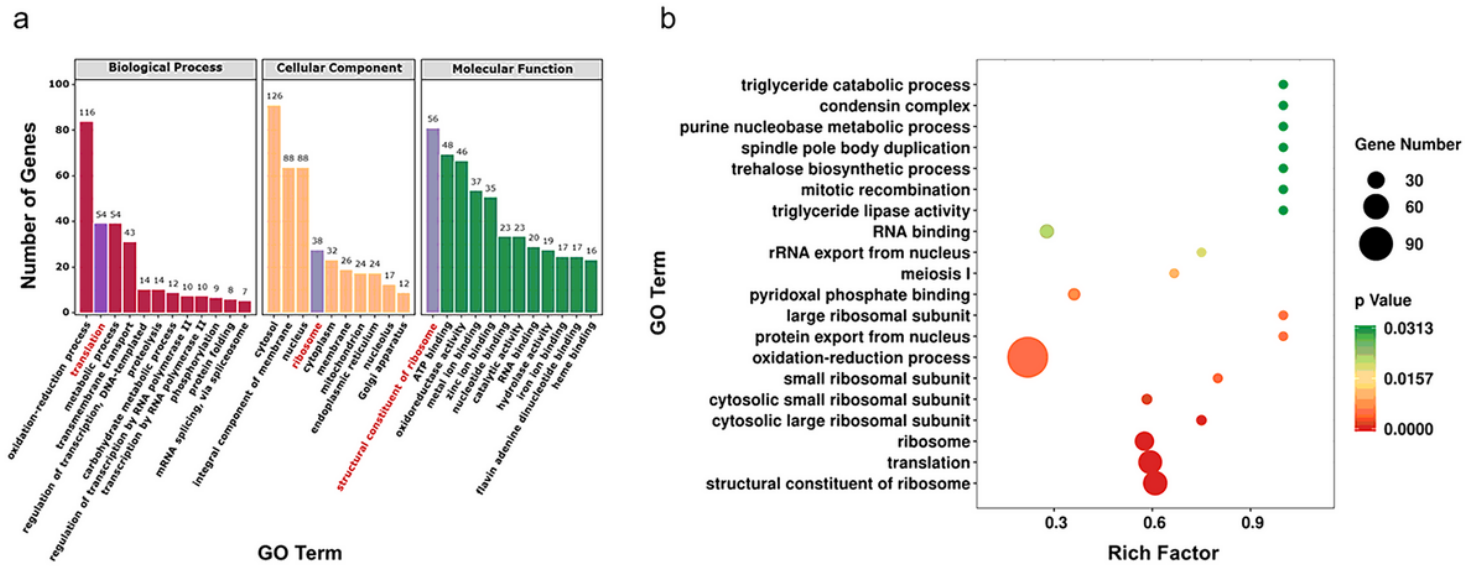

Figure 7

Gene Ontology (GO) analysis of the differentially expressed genes (DEGs) in Didymella segeticola. D. segeticola hyphae treated with Ningnanmycin (NNM), relative to control hyphae. GO functional classification of the DEGs. The number on the bar chart indicates the number of DEGs, and the ordinate indicates the percentage of DEGs of all the genes in this GO term (a). GO enrichment analysis of the DEGs. The higher the rich factor, the greater the degree of enrichment (b).

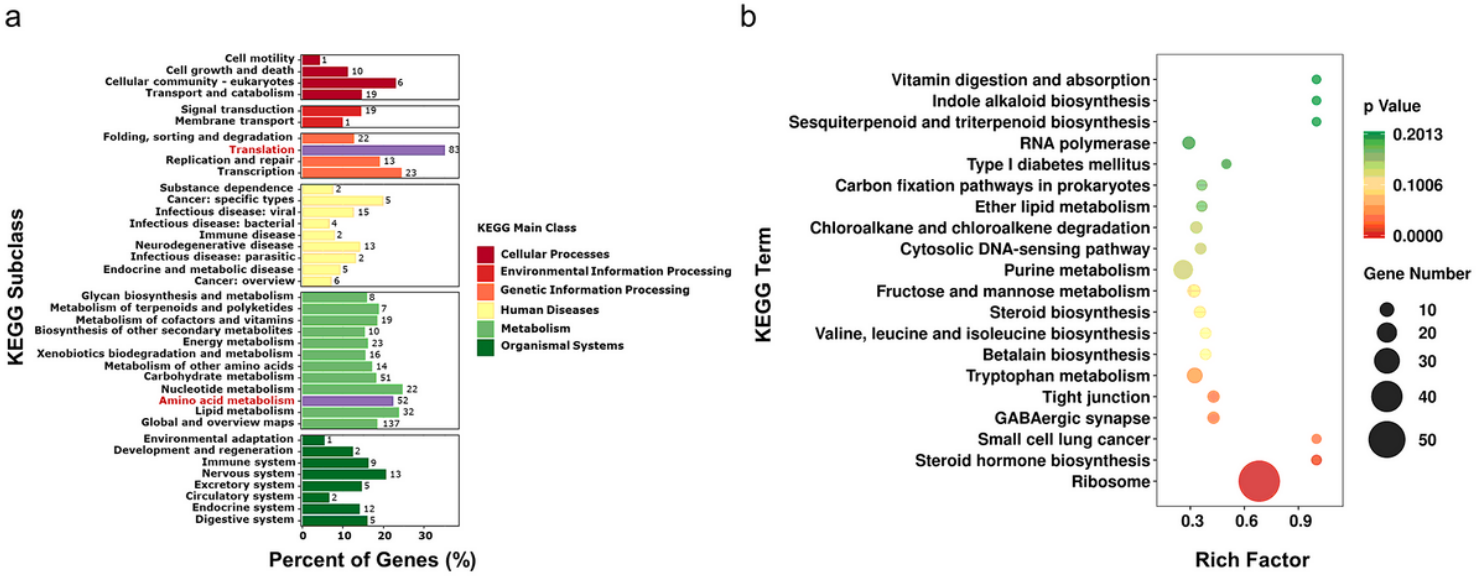

Figure 8

Kyoto Encyclopedia of Genes and Genomes (KEGG) analysis of the differentially expressed genes (DEGs). The DEGs of Didymella segeticola hyphae treated with Ningnanmycin (NNM), relative to control hyphae. KEGG subclass distribution of the DEGs. The number on the bar chart indicates the number of DEGs, and the abscissa indicates the percentage of the DEGs of all genes in this KEGG subclass (a);

KEGG enrichment analysis of the DEGs. The higher the rich factor value, the greater the enrichment of the pathway (b).

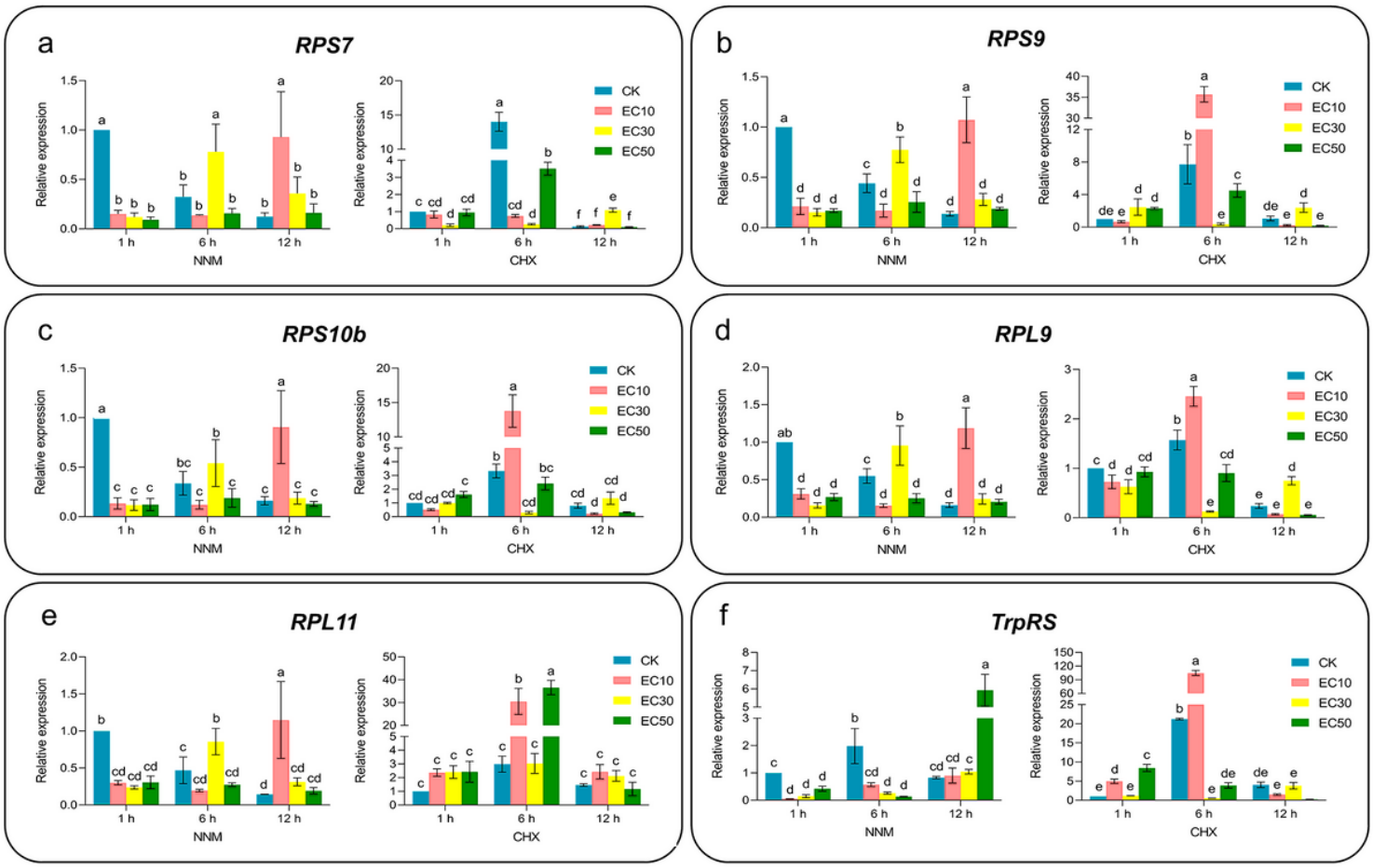

Figure 9

Expression levels of qPCR with six DEGs involved in translation process. 40S ribosomal protein S7 (RPS7) (a), 40S ribosomal protein S9 (RPS9) (b), 40S ribosomal protein S10b (RPS10b) (c), 60S ribosomal protein L9 (RPL9) (d), 60S ribosomal protein L11 (RPL11) (e) and tryptophanyl-tRNA synthetase (TrpRS) (f) of Didymella segeticola treated by Ningnanmycin (NNM) and cycloheximide (CHX) at three dosages and three states. Any two treatments with shared lowercase letters showed no significant difference at the level of $P < 0.05$. The error bar signifies “mean values ± standard error (SE)”.

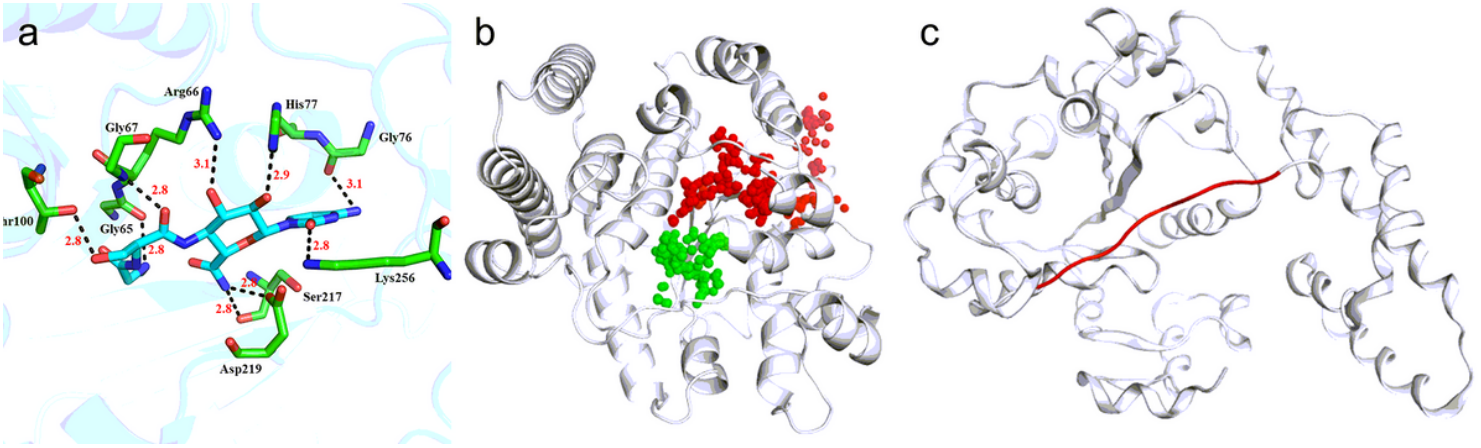

Figure 10

The proposed mode of interaction between Ningnanmycin (NNM) and tryptophanyl-tRNA synthetase (TrpRS) of Didymella segeticola. The proposed binding mode of NNM with TrpRS. The NNM and protein are shown in the purple and green stick model, respectively. The hydrogen bond is shown in black dashed lines (a); The most potent binding pockets of TrpRS (two pockets, red and green) (b); The template protein of TrpRS (c).

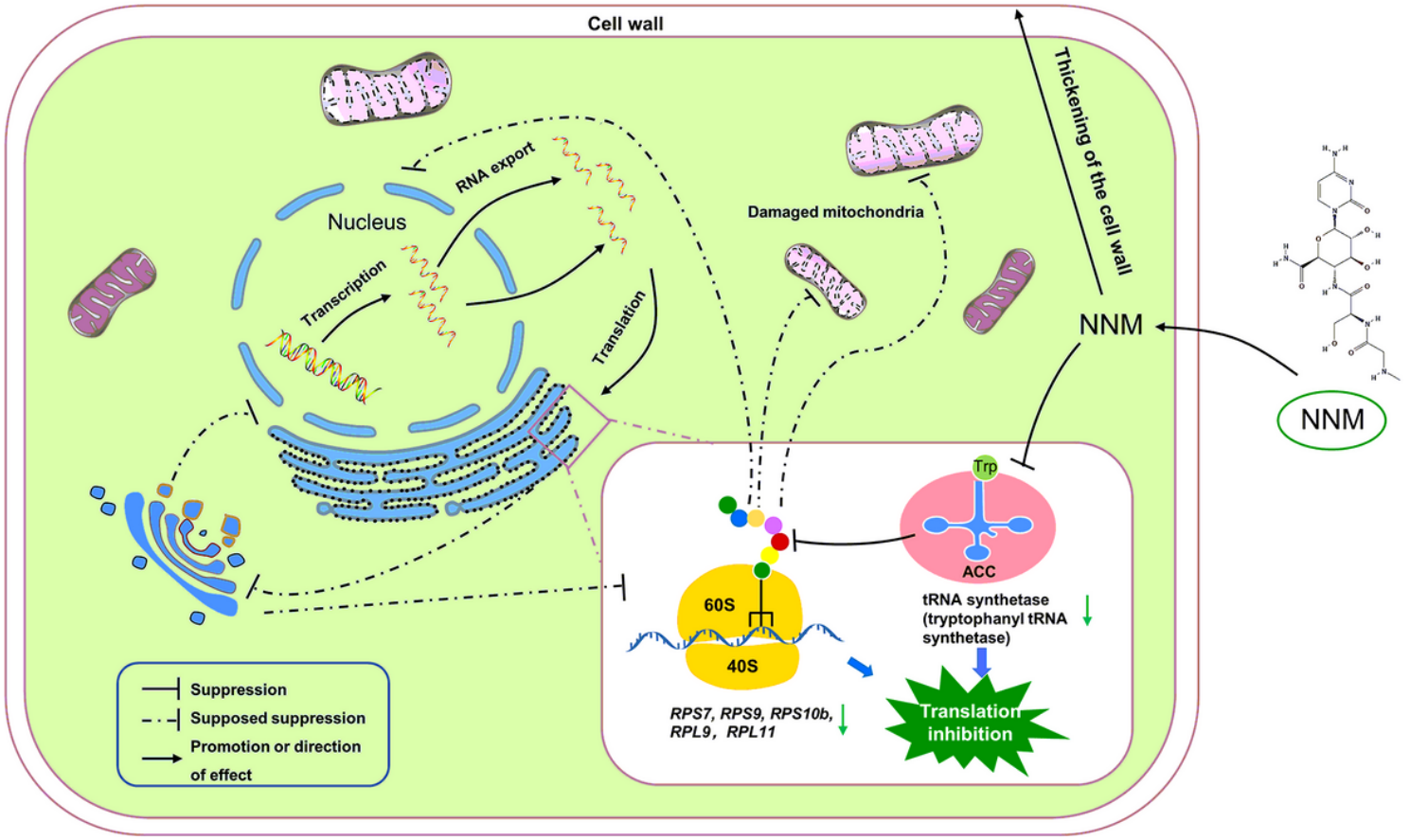

Figure 11

Hypothetical antifungal action model of Ningnanmycin (NNM) based on the results of our study. NNM initially down-regulated the expression levels of the translation-related genes, such as structural constituents of ribosomes and aminoacyl-tRNA synthases, involved in the translation process after NNM entered into the fungal hyphal cell. Moreover, NNM targeted tryptophan tRNA synthetase (TrpRS), thereby inhibiting the translation process. The growth of fungal hyphal cells was subsequently inhibited, with decreased density of the cytoplasm, reduced integrity of the mitochondria and thickening of the cell walls and septa. Furthermore, inhibition of translation might affect other enzymatic biological processes, such as DNA replication and transcription.

Supplementary Files

This is a list of supplementary files associated with this preprint. Click to download.

- Additionalfile1.docx
- Additionalfile2.docx
- Additionalfile3.docx
- Additionalfile4.xlsx